

The effects of oxidation temperature on the capacitance–voltage characteristics of oxidized AlN films on Si

J. Kolodzey,^{a)} E. A. Chowdhury, G. Qui, and J. Olowolafe

Department of Electrical and Computer Engineering, University of Delaware, Newark, Delaware 19716

C. P. Swann

Bartol Research Institute, University of Delaware, Newark, Delaware 19716

K. M. Unruh

Department of Physics and Astronomy, University of Delaware, Newark, Delaware 19716

J. Suehle

National Institute of Standards and Technology, Gaithersburg, Maryland 20899

R. G. Wilson

Hughes Research Laboratories, Malibu, California 90265

J. M. Zavada

ARO, Research Triangle Park, North Carolina 27709

(Received 10 October 1997; accepted for publication 29 October 1997)

The thermal oxidation of AlN thin films produces a high quality insulator which exhibits the gate voltage-controlled charge regimes of accumulation, depletion, and inversion on Si surfaces. The temperature dependence of oxidation is important for device processing. We report on the composition, structure, and electrical properties of the AlN versus the oxidization temperature. AlN layers 500 nm thick were deposited by rf sputtering on *p*-type Si (100) substrates, followed by oxidation in a furnace at temperatures from 800 to 1100 °C with O₂ flow. An oxidation time of 1 h produced layers of Al₂O₃ with small amounts of N having a thickness of 33 nm at 800 °C, and 524 nm at 1000 °C. Electrical measurements of metal-oxide-semiconductor capacitors indicated that the dielectric constant of the oxidized AlN was near 12. The best layer had a flatband voltage near zero with a net oxide trapped charge density less than 10¹¹ cm⁻². These results show that oxidized AlN has device-grade characteristics for the gate regions of field effect transistors, and for optoelectronic applications. © 1997 American Institute of Physics. [S0003-6951(97)04652-4]

High quality insulators such as thermally grown SiO₂ are crucial for optoelectronic device and circuit applications. The thickness of gate insulators in field effect transistors are being scaled to below 4 nm,¹ and tunneling leakage currents affect circuit operation and degrade reliability by time dependent dielectric breakdown.² Insulators with high dielectric constants can be made thicker for the same stored charge, producing a lower electric field and potentially fewer problems due to leakage and breakdown. Al₂O₃ has a high dielectric constant and may be an ideal alternative to SiO₂ depending on its properties.^{3–5} We have found that thermally oxidized AlN produces Al₂O₃ with excellent electrical and optical properties. In contrast, the oxidization of AlAs has also given interesting results,^{6,7} but this oxide may contain residual As, unlike oxidized AlN.

The oxidized AlN reported here was prepared using techniques described previously.⁵ Layers of AlN 500 nm thick were reactivity sputtered onto *p*-type Si (100) substrates, which were prepared by degreasing, an RCA etch, and an HF dip prior to sputtering. Oxidation was performed under dry O₂ flow in a quartz furnace tube at temperatures ranging from 800 to 1100 °C for durations of 1 and 2 h. The oxide structure was determined using $\theta/2\theta$ powder x-ray diffractometry (XRD). Figure 1 shows scans of XRD intensities over the angles associated with AlN and Al₂O₃ for a series of

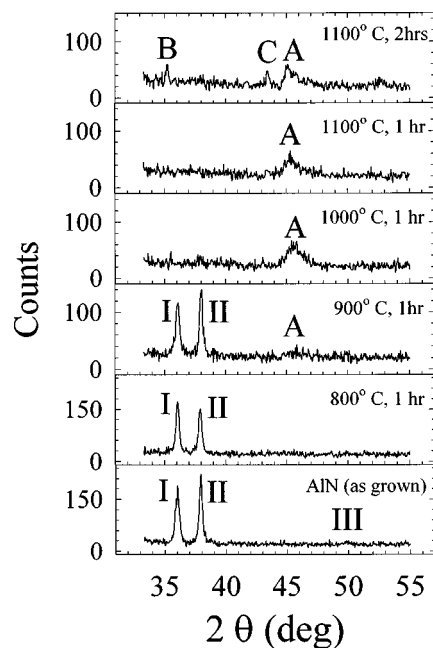


FIG. 1. XRD intensity vs scattering angle showing the trend of less AlN and more Al₂O₃ vs increasing oxidation temperature and time. The peak labels correspond reasonably to the angles expected for the following crystal phases and planes: (I) AlN (002); (II) AlN (101); (III) AlN (102); (A) θ -Al₂O₃ (several planes of the θ phase occur near this angle); (B) α -Al₂O₃ (104); (C) α -Al₂O₃ (113).

^{a)}Electronic mail: Kolodzey@ee.edel.edu

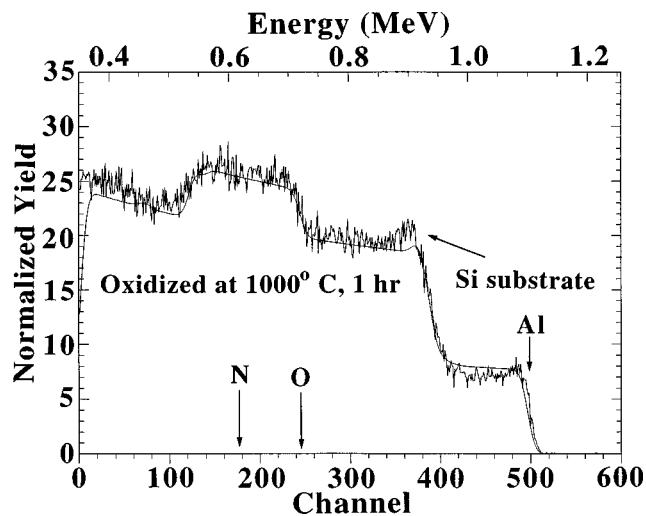


FIG. 2. RBS data of normalized ion counts vs ion energy using a 2.0 MeV He⁺ ion beam, for sample oxidized at 1000 °C. The spectrum shows Al at 1.1 MeV, Si from substrate at 0.9 MeV, and O from the Al₂O₃ at 0.7 MeV. If present, N would appear at 0.6 MeV. The smooth curve is the RUMP simulation which yielded the composition profiles vs temperature shown in Fig. 3.

oxidation temperatures and times. The presence of relatively weak multiple diffraction lines indicates that the as-deposited AlN and the oxidized layers consisted of amorphous and crystalline grains with several orientations. Several phases of Al₂O₃ were observed including sapphire (α -Al₂O₃). With increasing oxidation temperature and time, the XRD intensities of the AlN lines decreased and the intensities of the Al₂O₃ lines increased. The Al₂O₃ is evident at 1000 °C, and at 1100 °C there is little evidence for AlN. The XRD scans were made to reveal structure, however, and were not intended for revealing volume fractions of the compositions.

The layer compositions were measured using Rutherford backscattering spectrometry (RBS), and secondary ion mass spectrometry (SIMS). To estimate the composition versus depth, the RBS data were simulated using RUMP software.⁸ Figure 2 shows the RBS ion counts versus energy for a layer oxidized at 1000 °C, along with a RUMP simulation for a structure containing Al₂O₃ at the surface, a sublayer of unoxidized AlN, and a layer of SiO₂ next to the Si (to account for the possibility of oxidizing the Si substrate). For a simple estimate of the oxidation rates, we used RUMP simulations with only three abrupt layers having uniform, fixed compositions, with the layer thickness adjusted to minimize the simulation error. The simulations provided a reasonable match to the RBS data, and are in qualitative agreement with the SIMS results. The amount of N in the Al₂O₃ was estimated to be less than 10% because it was not detectable by RBS. In principle, more complicated simulations could be obtained by adding sublayers of intermediate compositions accounting for mixing at interfaces by interdiffusion and incomplete oxidation.

The thickness of the layers is plotted versus reciprocal temperature in Fig. 3, with an estimated accuracy of ± 3 nm. Straight lines on a log scale indicate thermally activated, diffusive behavior. The Al₂O₃ thickness slope yields 1.9 eV in the range between 900 °C and 1000 °C, which we interpret as the activation energy of AlN oxidation. By compari-

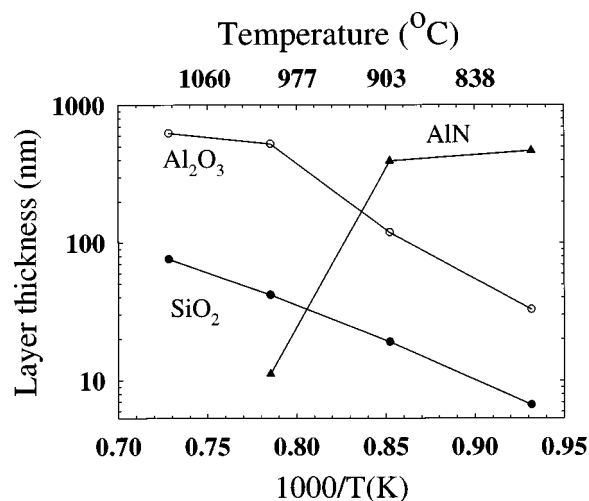


FIG. 3. Plot of layer thickness vs reciprocal temperature, based on RBS simulations using three layers. With increasing oxidation temperature, Al₂O₃ is grown at the expense of AlN (500 nm as-grown thickness). The Al₂O₃ growth is thermally activated as discussed.

son, the dry oxidation thickness of Si has activation energies of 1.24 eV in the diffusion-limited regime, and 2.0 eV in the linear regime.⁹ For temperatures less than 1100 °C, the presence of the SiO₂ layer is interpreted as an artifact of the simulation which attempted to minimize the error using only three layers in the presence of composition mixing, and is not considered to be physically real. RBS indicated that the oxidation of the AlN began at 800 °C. No unoxidized AlN remained above 1000 °C for a 500 nm layer, and our results indicate that a 120 nm layer of AlN would fully oxidize at 900 °C for 1 h. At 1100 °C, some SiO₂ was produced at the Si surface, showing that the Al₂O₃ layer was not a barrier to Si oxidation at this temperature. The RBS compositions versus temperature were reasonably consistent with the x-ray results of Fig. 1.

To measure the dielectric properties of the oxidized AlN insulator, metal-insulator-silicon (MIS) capacitors were fabricated and measured versus bias and frequency.¹⁰ Electrical contacts of Al metal 100 nm thick were sputtered onto the top of the oxide and the bottom of the Si substrate. The top contacts were patterned by conventional photolithographic liftoff into arrays of circular dots of area 8×10^{-4} cm². As shown in Fig. 4, the capacitance–voltage C – V characteristics indicated that the gate bias brought the Si surface charge into the regimes of accumulation at negative gate voltages, and depletion and inversion at progressively more positive voltages. This is similar to the well known behavior of SiO₂ capacitors.⁹ The surface inversion at measurement frequencies below 1 MHz is pivotal for transistor operation because it indicates that there are no defects which pin the Fermi level near mid-gap and prevent the appearance of mobile electrons at the Si surface. At frequencies higher than the carrier thermal generation rate (near 1 MHz), the semiconductor remains depleted with correspondingly lower capacitance.

The C – V data are summarized in Table I. The flatband voltage is:

$$V_{\text{FB}} = \Phi_{\text{MS}} - Q_{\text{OX}} / C_{\text{OX}},$$

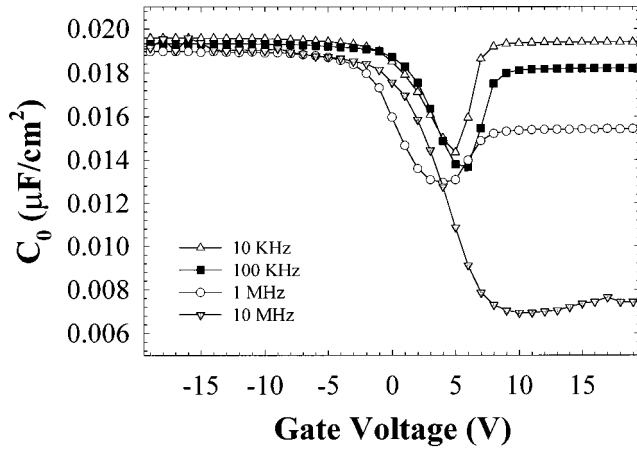


FIG. 4. Capacitance–voltage characteristics vs frequency for AlN oxidized at 1000 °C for 1 h. Surface charge inversion of the Si occurs for positive bias at frequencies below 1 MHz.

where Φ_{MS} is the metal–semiconductor work function difference (near -0.9 V for Al metal and p -type Si), Q_{OX} is the net oxide trapped charge (the first moment of the oxide charge distribution divided by the oxide thickness), and C_{OX} is the capacitance of the oxide layer. Samples oxidized at 1000 °C and above have Q_{OX}/q near 10^{11} cm^{-2} , which is comparable to that of device-grade SiO_2 .⁹ Lower temperatures yielded higher values of V_{FB} and Q_{OX} which were attributed to the presence of unoxidized AlN, because we observed that thinner samples in which the AlN was fully oxidized at 900 °C had low defect densities. We emphasize that Q_{OX} includes contributions from the entire oxidized layer, and would not be reduced merely by the presence of defect-free SiO_2 at the Si interface.

The effective dielectric constant of the oxide κ_{OX} , given in Table I, was obtained from the capacitance measurements. These values are comparable to the values for α - Al_2O_3 ($\kappa_{\text{sapphire}} = 12$),¹¹ and unoxidized AlN ($\kappa_{\text{AlN}} = 9.14$)¹² which

TABLE I. The dielectric properties of oxidized AlN thin films from C – V measurements of MIS capacitors. The sublayer thickness was determined from RUMP software simulations to the RBS data, assuming a three layer structure. The as-grown AlN was near 500 nm thick for all samples. The sample number, oxidation temperature and time, dielectric constant, net oxide trapped charge, and flatband voltage are indicated.

Sample	T_{OX}/d_{OX} (°C/h)	κ_{OX}	Q_{OX}/q (cm^{-2})	V_{FB} (V)
100601a	1100/2	10	5.56×10^{10}	-1.67
100601b	1100/1	8.6	1.36×10^{11}	-2.96
100601c	1000/1	12.6	2.5×10^{11}	$+1.13$
100601d	900/1	15.6	2.84×10^{12}	-18.1
100601e	800/1	14.2	2.85×10^{12}	-19.4

are significantly higher than the value of 3.9 for SiO_2 . The reason for the increase in κ_{OX} as temperature decreased is not yet clear, but may be partly due to thickness errors. The sample oxidized at 1000 °C had an oxide leakage current density of 1.2×10^{-7} A cm^{-2} at a field of 1 MV/cm, corresponding to a resistance of 5.8×10^{11} Ω .

These results show that AlN thin films on Si can be oxidized at standard process temperatures, producing a device-grade insulator with sufficient quality for the gates of field effect transistors. The oxidation produced Al_2O_3 with no N detected by RBS. C – V measurements of MIS capacitors on Si exhibited surface charge inversion, showing that oxidized AlN has low defect densities and is comparable to device-grade SiO_2 . The dielectric constant is higher than that of SiO_2 , and oxidized AlN can be used as a thicker gate insulator for Si-based field effect transistors with less tunneling leakage and greater reliability for the same stored charge. Other possible applications include native oxides for AlGaN-based MIS field effect transistors, and dielectrics for optical devices.

Special thanks go to Dave Smith for valuable advice and help with metallization, to Y. Chen for help with the C – V measurements, and to Dr. J. Comas for valuable advice. This work was supported by the ARO under Grant No. DAAH04-95-1-0625, and DARPA under Contract No. F49620-96-C-0006.

¹C. Hu, Tech. Dig. Int. Electron Devices Meet., 319 (1996).

²A. Martin, J. Suehle, P. Chaparala, P. O’Sullivan, and A. Mathewson, Proceedings of the 1996 International Reliability Physics Symposium, April 30–May 2, 1996, Dallas, pp. 67–76; M. Nafria, J. Sune, D. Yelamos, and X. Aymerich, IEEE Trans. Electron Devices **43**, 2215 (1996).

³F. Ansart, H. Ganda, R. Saporte, and J. P. Traverse, Thin Solid Films **260**, 38 (1995).

⁴See *Oxides and Oxide Films*, edited by J. W. Diggle and A. K. Vijh (Marce–Dekker, New York, 1976), Vol. 4; G. T. Cheney, R. M. Jacobs, H. W. Korb, H. E. Nigh and J. Stack, Proceedings of IEEE Device Meeting, Oct. 18–21, 1967, Washington D.C., paper 2.2.

⁵E. A. Chowdhury, J. Kolodzey, J. Olowolafe, G. Qui, G. Katulka, D. Hits, M. Dashiell, D. van der Weide, C. P. Swann, and K. M. Unruh, Appl. Phys. Lett. **70**, 2732 (1997).

⁶M. J. Ries, N. Holonyak, Jr., E. I. Chen, and S. A. Maranowski, Appl. Phys. Lett. **67**, 1107 (1995).

⁷E. F. Schubert, M. Passlack, M. Hong, J. Mannerts, R. L. Opila, L. N. Pfeiffer, K. W. West, C. G. Bethea, and G. J. Zydzik, Appl. Phys. Lett. **64**, 2976 (1994).

⁸L. R. Doolittle, Nucl. Instrum. Methods Phys. Res. B **9**, 344 (1985).

⁹E. H. Nicollian and J. R. Brews, *MOS Physics and Technology* (Wiley-Interscience, New York, 1982).

¹⁰J. Suehle, P. Chaparala, C. Messick, W. M. Miller, and K. C. Boyko, Proceedings of the 1994 Reliability Physics Symposium, April 12–14, 1994, San Jose, pp. 120–125.

¹¹The dielectric constant of α - Al_2O_3 has components 11.5 and 9.65 parallel and perpendicular to the c axis, respectively, at the frequency of 10^6 Hz at 298 K; *Hand Book of Thin Film Technology*, edited by L. I. Maissel and R. Glang (McGraw-Hill, reissue, New York, 1983), pp. 6–12.

¹²*Semiconductors—Basic Data*, edited by O. Madelung (Springer, Berlin, 1991).